# High Precision Phase Noise Analysis Based on a Photonic-Assisted Microwave Phase Shifter Without Nonlinear Phase Distortion

Jian Wang , Wenting Wang , Renheng Zhang , Bei Chen , Dechao Ban , Ya Jin , Keqi Cao, Yu Liu , and Ninghua Zhu

*Abstract*—We propose and demonstrate a high-precision phase noise analysis method based on a photonic-assisted microwave phase shifter (MPS) without nonlinear phase distortions (NPD). The proposed scheme utilizes a dual parallel Mach Zehnder modulator (DPMZM) and an optical bandpass filter (OBPF) to implement the photon-assisted microwave phase shifter. To avoid additional frequency noise induced by frequency fluctuations of the optical carrier, we employ a dispersion compensation photonic delay line as the delay line component. The MPS operates in the optical single sideband modulation (OSSB) mode with even-order sideband suppression, allowing continuous phase tuning over the entire 360° range and eliminating NPD commonly encountered in traditional microwave photonic phase shifters. Experimental results demonstrate significant improvements in the phase and magnitude responses of the MPS without NPD compared to those with NPD. The proposed system exhibits long-term stability, with phase drift and amplitude drift of less than 5° and 1 dB, respectively, over continuous operation for more than 1500 seconds. We successfully measured microwave signals at the frequency of 8 GHz, 10 GHz, and 12 GHz with phase noise of −66.7, −65.5, and −62.1 dBc/Hz at 10 kHz offset frequency without resetting the proposed system. The method could be used to characterize electronic and photonic oscillators, which is highly reconfigurable and widely tunable.

Jian Wang, Renheng Zhang, and Keqi Cao are with the State Key Laboratory of Integrated Optoelectronics, Institute of Semiconductors, Chinese Academy of Sciences, Beijing 100083, China, and also with the University of Chinese Academy of Sciences, Beijing 100049, China (e-mail: wangjian@semi.ac.cn; renhengzhang@126.com; keqicao@semi.ac.cn).

Wenting Wang is with the Communication and Integrated Photonics Laboratory, Xiongan Institute of Innovation, Chinese Academy of Sciences, Xiong'an New Area 071000, China (e-mail: wenting.wang@xii.ac.cn).

Bei Chen, Dechao Ban, Ya Jin, and Yu Liu are with the State Key Laboratory of Integrated Optoelectronics, Institute of Semiconductors, Chinese Academy of Sciences, Beijing 100083, China (e-mail: beichen@semi.ac.cn; dchban@semi.ac.cn; jinya@semi.ac.cn; yliu@semi.ac.cn).

Ninghua Zhu is with the State Key Laboratory of Integrated Optoelectronics, Institute of Semiconductors, Chinese Academy of Sciences, Beijing 100083, China, and with the University of Chinese Academy of Sciences, Beijing 100049, China, and also with the Communication and Integrated Photonics Laboratory, Xiongan Institute of Innovation, Chinese Academy of Sciences, Xiong'an New Area 071000, China (e-mail: nhzhu@semi.ac.cn).

Digital Object Identifier 10.1109/JPHOT.2023.3314761

## I. INTRODUCTION

**P**HASE noise is one of the most critical parameters used to evaluate the performance of microwave signal sources, as it represents the short-term frequency stability of the signal [1], [2]. In fields such as radar, communication, measurement, and navigation, there is a high demand for microwave signal sources with low phase noise [3], [4], [5], [6]. The development of ultra-low phase noise microwave signal sources has created an urgent need for high-precision phase noise analysis. In the past few decades, three techniques have been proposed to measure the phase noise of microwave signals [7], each with its own set of advantages and disadvantages. The first and most straightforward method is to use a spectrum analyzer (SA) to directly measure the power spectral density (PSD) of the oscillator. However, this method has limited accuracy and dynamic range, typically less than 100 dB, due to the bandwidth of the intermediate frequency (IF) filter within the SA and its own LO phase noise [8]. To overcome these limitations, a mixer-based phase detector is used to convert phase fluctuations into baseband voltage fluctuations. Heterodyne measurement, which involves a phase detector and a phase-locked loop (PLL), is a promising method. For the mixer to function as a phase detector, the two input signals should have a 90° phase difference. This method can measure phase noise with high precision, but it requires an extra reference oscillator with better performance than the oscillator under test and frequency tunability [9]. However, the locking bandwidth of the PLL limits the lower Fourier offset frequency from the carrier, although its upper Fourier offset frequency can be expanded up to the Nyquist frequency of the oscillator. As a result, homodyne techniques without a PLL based on a delay line and a phase detector have been proposed for phase noise measurement. This method's key advantage is that it does not require an additional reference oscillator and does not have a lower offset frequency from the carrier. Therefore, it can be used to measure long-term stability over periods greater than 1 s (less than 1 Hz from the carrier in the frequency domain) with the assistance of data acquisition (DAQ) [10]. Its primary disadvantage is that it has an upper offset frequency limit determined by the frequency response of the delay line. In this scheme, a microwave signal from an oscillator is split into two parts, and a relative time delay and phase shift between them are introduced to achieve decorrelation and ensure the mixer acts as a phase detector. As

oscillator performance continues to improve, the corresponding delay-line-based scheme requires a longer delay time, which is a significant challenge for electrical techniques. Additionally, the phase detector requires a phase shifter with a wider operational bandwidth to introduce an exact $90°$ phase difference.

Optical techniques have emerged as a potential solution to overcome these limitations. Several optical schemes have been proposed for phase noise measurement, such as using an optical fiber as a delay line to enhance sensitivity and precision [9]. However, the performance of these systems may still be limited by complicated electrical processing units. Optical frequency comb and carrier suppression interferometer techniques have been introduced to enhance measurement sensitivity [11], [12]. To eliminate the calibration procedure, quadrature phase demodulation based on in-phase and quadrature (I/Q) mixing and digital signal processing have been adopted [13], [14], [15]. To further reduce the requirements for electrical processing modules and expand the system's operating bandwidth, photonic-assisted microwave processors have been introduced into the phase noise measurement system [16], [17], [18], [19], [20], [21], [22]. These processors use microwave photonic technologies to achieve bandwidth enhancement for microwave phase shifting or frequency mixing. For example, in [21], an electro-optical polarization modulator (PolM) was used to realize phase shifting. However, the system based on a polarization modulator is extremely sensitive to the surrounding environment, making it unreliable for realistic applications [22], [23]. In another study [18], a dual-drive Mach-Zehnder modulator was utilized to upconvert the low-frequency signal to a higher frequency. This approach effectively expanded the operational bandwidth of the system at lower frequencies to 0.5 GHz. In [11], a compact phase noise measurement system was achieved by substituting an electroabsorption modulated laser for the laser source and intensity modulator in the photon delay method. However, these approaches did not take into consideration the non-linear phase distortion (NPD) introduced by the beat frequency between adjacent high-order sidebands.

In this article, we propose a high precision phase noise analysis method based on a photonic-assisted microwave phase shifter (MPS) without nonlinear phase distortion (NPD) combined with an optical fiber delay line. The proposed system could work over a wide frequency range without reconfiguration and under complicated electromagnetic environment [24], [25], [26]. It not only saves the use of a MPS, but also effectively stretches the delay line in the conventional delay line phase noise measurement system. A particularly desirable feature of this approach is that the NPD is considerably suppressed in the photonic-assisted MPS which may contaminate noise property of oscillators under test resulting in a phase noise measurement error. In this scheme, by properly setting the bias voltages of a dual-parallel Mach-Zehnder modulator (DPMZM), the NPD of the photonic-assisted MPS could be eliminated to avoid phase noise measurement error. Microwave signals over a wide frequency range from 8 GHz to 40 GHz could be phase shifted over a full $360°$ within a magnitude variation of 4 dB. Moreover, the long-term stability of the photonic-assisted MPS is also experimentally investigated. A proof-of-concept experiment is
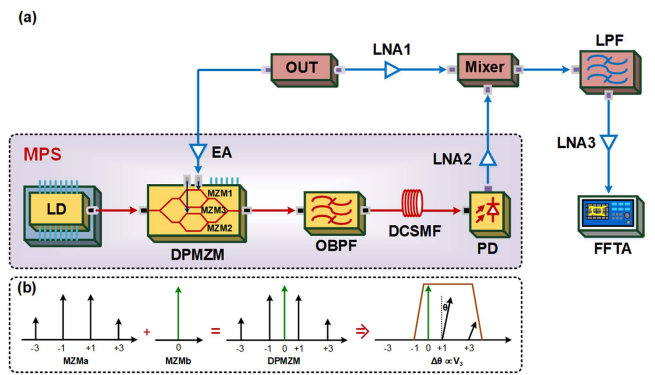


Fig. 1. (a) Schematic diagram of the proposed high precision phase noise analysis method (LD: laser diode; DPMZM: phase modulator; OBPF: optical bandpass filter; DCSMF: dispersion compensated single mode fiber; PD: photodetector; EA: electrical amplifier; LNA: low noise amplifier; LPF: low-pass filter; OUT: oscillator under test; FFTA: fast Fourier transform analyzer); (b) schematics of optical spectra after each device.

carried out to verify the proposed method. The experimental results confirm that the proposed method is feasible.

## II. PRINCIPLE

The schematic configuration of the proposed phase noise analysis method without phase noise measurement errors based on a photonic-assisted MPS using a DPMZM and dispersion compensated single mode fiber (DCSMF) acting as a photonic delay line is illustrated in Fig. 1. An optical carrier from a narrow linewidth laser diode (LD) with an angular frequency of $\omega_c$ is fiber-coupled to a DPMZM via a polarization controller (PC) which is used to minimize a polarization dependence loss (PDL). The microwave signal from an oscillator under test (OUT) is divided into two parts by splitting ratio of 1:1. One part is boosted by an electrical amplifier (EA) to drive one of arms of DPMZM and the other part is amplified by a low noise amplifier (LNA) to act as a reference signal for a phase detector. The phase detector comprises a double balanced passive mixer, a low-pass filter (LPF), and LNA3 as shown in the inset of Fig. 1. MZM1 and MZM2 setting in parallel compose the DPMZM, which contains three DC biases and two RF input ports. An optical single sideband (OSSB) modulation with even-order sidebands suppression is realized by removing either sideband of the optical carrier with an optical bandpass filter (OBPF). It not only avoids power fading but also achieves the MPS. By properly adjusting bias voltages of DPMZM, a relative phase difference between two optical sidebands is continuously changed. The OSSB modulated optical signal is sent into the DCSMF to achieve a transformation from frequency fluctuations into phase fluctuations ($\Delta\omega \rightarrow \Delta\varphi$). As the frequency slightly changes, the corresponding phase ($\varphi = \omega t$) happening in the DCSMF will be proportionally changed. Therefore, it is more desirable to use a temperature stabilizing DCSMF acting as a photonic delay line. Meanwhile, the delay time should be as large as possible so that even quite small frequency fluctuations can be extracted. The optical signals undergo a delay of the DCSMF and then are converted into a microwave signal in a photodetector (PD).

The phase shifted and time delayed microwave signal is amplified by a LNA2 and is injected into another port of the phase detector to obtain the other conversion from phase fluctuations into baseband voltage fluctuations ($\Delta\varphi \rightarrow \Delta V$). The two signals launched into two ports of the phase detector must require a $90°$ phase difference, and the output voltage fluctuations are proportional to the input phase fluctuations. The baseband voltage fluctuations are recorded using a fast Fourier transform analyzer (FFTA).

We suppose the optical carrier has a normalized electrical field expressed as $E_{In}(t) = exp(j\omega_c t)$. The MZM1 is driven by a microwave signal with an electrical field of $(V_{RF1} + \Delta V_{RF1}(t)) \times cos(\omega_{RF1}t + \varphi_1 + \Delta\varphi(t))$, where $V_{RF1}$, $\omega_{RF1}$, and $\varphi_1$ are the magnitude, angular frequency, and fixed phase. $\Delta V_{RF1}$ and $\Delta\varphi(t) = \Delta\omega_{RF1}t$ are magnitude fluctuations and phase fluctuations of microwave signals under test, where $\Delta\omega_{RF1}$ is frequency fluctuations or linewidth of the microwave signal. In order to flexibly control the optical carrier power, the MZM2 is not driven by a microwave signal and let the optical carrier go through. Therefore, the electrical filed at the DPMZM output could be written as:

$$
\begin{aligned}
&E_{Out}(t) \\
&= [E_{MZM1}(t)\exp(j\theta_3) + E_{MZM2}(t)]/\sqrt{2} \\
&= E_{In}(t)\cos(\beta\cos(\omega_{RF1}t + \varphi_1 + \Delta\varphi(t)) + \theta_1/2) \\
&\quad \cdot \exp(j\theta_3)/2 + E_{In}(t)\cos(\theta_2/2)/2
\end{aligned} \quad (1)
$$

where $E_{MZM1}$ and $E_{MZM2}$ are the electrical field at MZM1 and MZM2 output, $\theta_n = \pi V_n/V_\pi (n = 1, 2)$ are the phase shift controlled by the DC biases voltages of two sub-MZMs, $V_n$ is the DC bias voltages, $\beta = \pi(V_{RF1} + \Delta V_{RF1})/V_\pi$ is the modulation index, and $V_\pi$ is a half-wave voltage of MZM1. $\theta_3 = \pi V_3/V_{\pi-DP}$ is a relative phase difference between two sub-MZMs, $V_{\pi-DP}$ is the half-wave voltage of the parent MZM. Applying Jacobi-Anger expansion to (1) and considering large signal modulation by increasing microwave signal power, we could get the electrical field at the DPMZM output as follow:

$$
\begin{aligned}
&E_{Out}(t) \\
&= E_{In}(t)\left\{E_0 + \cos(\theta_1/2)\sum_{n=-\infty}^{\infty}(-1)^n \right. \\
&\quad \cdot J_{2n}(\beta)\exp[j(2n(\omega_{RF1}t + \varphi_1 + \Delta\varphi(t)) + \theta_3)] \\
&\quad - \sin(\theta_1/2)\sum_{-\infty}^{\infty}(-1)^n J_{2n-1}(\beta)\exp[j \\
&\quad \left. \cdot((2n-1)\cdot(\omega_{RF1}t + \varphi_1 + \Delta\varphi(t)) + \theta_3)]\right\}/2
\end{aligned} \quad (2)
$$

where $E_0 = J_0(\beta)\cos(\theta_1/2)\exp(j\theta_3) + \cos(\theta_2/2)$. Then, the optical signal goes through an OBPF to remove optical sidebands either side of the optical carrier to get OSSB modulated signals. Meanwhile, the optical signals pass through the DCSMF to introduce a time delay $\tau$. Therefore, the electrical field at the DCSMF output could be rewritten as follow:

$$
\begin{aligned}
&E_{Out}(t) = E_{In}(t-\tau)\left\{E_0 + \cos(\theta_1/2)\sum_{n=0}^{\infty}(-1)^n J_{2n}(\beta) \right. \\
&\quad \cdot \exp[j(2n(\omega_{RF1}(t-\tau) + \varphi_1 + \Delta\varphi(\tau)) + \theta_3)] \\
&\quad - \sin(\theta_1/2)\sum_{n=0}^{\infty}(-1)^n J_{2n-1}(\beta)\exp[j((2n-1) \\
&\quad \left. \cdot(\omega_{RF1}(t-\tau) + \varphi_1 + \Delta\varphi(\tau)) + \theta_3)]\right\}/2
\end{aligned} \quad (3)
$$

As can be seen from (3), we could clearly observe that frequency fluctuations could be proportionally converted into phase fluctuations with a relationship of $\Delta\omega_{RF1} \times \tau = \Delta\varphi(\tau)$. After a square-law detection in a PD, the output photocurrent $I(t)$ is given as

$$
I(t) = A_0(t) + A(t) + B(t) + C(t) + \ldots \quad (4)
$$

where $A_0(t)$ is the desirable microwave signal with the angular frequency of $\omega_{RF1}$ recovered from the modulated optical signal, $A(t)$ results from the higher-order sidebands to the magnitude and phase of the recovered microwave signal with a fundamental frequency, which will induce the NPD. These nonlinear distortions are an origin of phase noise measurement error, $B(t)$ is the unwanted second harmonics which also will be injected into the phase detector to introduce some phase noise measurement errors, and $C(t)$ is the corresponding third harmonics. These high harmonic signals will be underlying mixed with each other in the mixer to generate phase noise measurement errors.

$$
\begin{aligned}
A_0(t) &= E_0\sin(\theta_1/2)J_1(\beta) \quad (5a) \\
&\quad \cdot \exp\{-j[\omega_{RF1}(t-\tau) + \varphi_1 + \Delta\varphi(\tau) + \theta_3]\}/2 \\
&\quad + E_0^*\sin(\theta_1/2)J_1(\beta) \\
&\quad \cdot \exp\{j[\omega_{RF1}(t-\tau) + \varphi_1 + \Delta\varphi(\tau) + \theta_3]\}/2
\end{aligned}
$$

$$
\begin{aligned}
A(t) &= -\sin\theta_1\sum_{n=1}^{\infty}J_n(\beta)J_{n+1}(\beta) \quad (5b) \\
&\quad \cdot \cos[\omega_{RF1}(t-\tau) + \varphi_1 + \Delta\varphi(\tau) + \theta_3]/2
\end{aligned}
$$

$$
\begin{aligned}
B(t) &= B_0(t) - \frac{\sin^2(\theta_1/2)}{2}\sum_{n=1}^{\infty}J_n(\beta)J_{n+2}(\beta) \quad (5c) \\
&\quad \cdot \cos[2(\omega_{RF1}(t-\tau) + \varphi_1 + \Delta\varphi(\tau)) + \theta_3]
\end{aligned}
$$

$$
\begin{aligned}
C(t) &= C_0(t) - \sin\theta_1\sum_{n=1}^{\infty}J_n(\beta)J_{n+3}(\beta) \quad (5d) \\
&\quad \cdot \cos[3(\omega_{RF1}(t-\tau) + \varphi_1 + \Delta\varphi(\tau)) + \theta_3]/2
\end{aligned}
$$

As can be seen from (5b), some main measurement errors are introduced into the system to additionally degrade the quality of microwave signal because of the beating between any two adjacent higher-order sidebands. In order to remove the NPD and effectively expand dynamic range of the proposed system, MZM1 is biased at the minimum transmission point (MITP) and MZM2 is biased at the maximum transmission point (MATP).
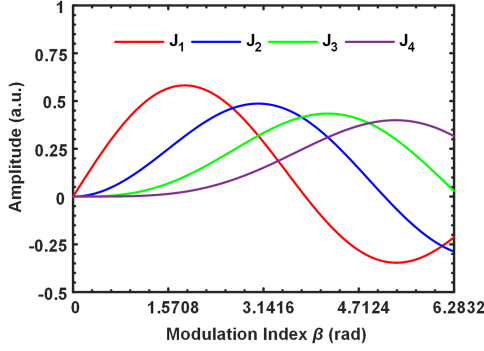
Fig. 2.  Variations of $J_1(\beta)$, $J_2(\beta)$, $J_3(\beta)$ and $J_4(\beta)$ versus $\beta$.

Therefore, we firstly tune the bias voltages of the MZM1 to suppress even-order sidebands so that $\theta_1 = \pi$ and $V_1 = V_\pi$. We could firstly obtain $E_0 = E_0^*$, $A(t) = 0$, $C(t) = C0(t)$. It is obviously observed that the power of the second harmonic signal depends on Bessel coefficients of $J_n(\beta)$ and $J_{n+2}(\beta)$. Therefore, we make a simulation to observe the amplitude variation of higher order sidebands varying with modulation index $\beta$ as shown in Fig. 2. The amplitude of the first-order sideband is proportional to $J_1(\beta)$ based on the simulation, which monotonically increases over a range of $0 \leq \beta \leq 1.86$. It is clearly shown that the amplitude of the first-order sideband reaches a peak when the modulation index equals 1.86 rd. In order to remove measurement errors induced by higher harmonics shown in (5c) and (5d), the microwave signal power fed into the MZM1 is adjusted to meet the requirement of $\beta = 1.86$. Therefore, the power of the driven microwave signal of the DPMZM is considered to be $(1.86V_\pi/\pi)^2/50$. In our scheme, the corresponding microwave signal power is about 175 mW. We could achieve $A(t) = 0$, $B(t) \approx 0$, $C(t) = 0$. Therefore, we could get pure microwave signals at the PD output without the NPD and higher order harmonics as follows:

$$A_0(t) = \cos\frac{\theta_2}{2} J_1(\beta) \cos(\omega_{RF1}(t - \tau) + \varphi_1 + \Delta\varphi(\tau) + \theta_3)$$
(6)

As can be seen from (6), $\varphi_1$ and $\omega_{RF1}\tau$ are stable phases introduced by the driven microwave signal and the delay time. We suppose the delay line is stable. That is, the length the photonic delay line is stabilized. In this scheme, we make use of a DC-SMF to avoid additional frequency noise induced by frequency fluctuations of the optical carrier. In essence, the linewidth of LD will introduce some extra frequency noise. Therefore, we tune the bias voltage $V_3$ to achieve phase shift for the microwave signals under test. We could obtain $\omega_{RF1}\tau + \varphi_1 + \theta_3 = \pi/2$ by adjusting the bias voltages $V_3$. Meanwhile, we adjust the bias voltage of the MZM2 to improve the optical carrier to sideband ratio (OCSR) to optimal sensitivity of the system. It is worth noting that the optical carrier power is governed by the transfer function of the MZM2. The generated microwave signal is mixed with a reference signal in a mixer, in which a sum frequency ($2\omega_{RF1}$) is filtered off with a low-pass filter attached after it retaining the difference frequency. We could get voltage

fluctuations as follow:

$$\Delta V(t) \propto \alpha \left[V_{RF1} + \Delta V_{RF1}(t)\right] \cos(\theta_2/2) J_1(\beta)$$
$$\cdot G_1 G_2 \sin(\Delta\omega_{RF1}\tau)$$
(7)

where $\alpha(V^{-1})$ is the conversion efficiency of the mixer, and G1, G2 are gain coefficients of LNA1 and LNA2, respectively. Considering phase noise of the OUT with much less than 1 rd, we could define the phase detection sensitivity $K_\varphi$ (V/rad) of the phase detector as follow:

$$K_\varphi = \frac{\Delta V(t)}{\Delta\omega_{RF1}\tau} \propto \alpha \left[V_{RF1} + \Delta V_{RF1}(t)\right] \cos\frac{\theta_2}{2} J_1(\beta)G_1G_2$$
(8)

It is clearly shown that RIN of OUT will introduce some phase noise measurement errors. RIN of the microwave signal is firstly coupled into the modulation index $\beta$ and then further contaminate phase noise in the process of phase detection. In our scheme, we assume that the RIN of the microwave signal could be neglected. In general, phase noise with a mirror image is quantified in terms of two-sided PSD $S_\varphi(f)$ of the carrier for phase fluctuations in a unit of $[\text{rad}^2/\text{Hz}]$, as a function of Fourier frequency $f$. We could get two-sided PSD as follow:

$$S_\varphi(f) = \frac{P_\varphi(f)}{4K_\varphi^2 \sin^2(\pi f \tau)}$$
(9)

where $P_\varphi(f)$ is the PSD for voltage fluctuations in a unit of $[\text{V}^2/\text{Hz}]$ measured by the FFTA. Therefore, with an assist of the phase detection sensitivity $K_\varphi$, we could convert $[\text{V}^2/\text{Hz}]$ into $[\text{rad}^2/\text{Hz}]$. When the phase fluctuation is much less than $2\pi$, the unit for $S_\varphi(f)$ could be changed into [dBc/Hz] with a relation of $10\log_{10}(S_\varphi(f))$. Phase noise measurement could be regarded as a two steps process, first converting the frequency fluctuations into phase fluctuations with a photonic delay line, and then converting the phase fluctuations into voltages fluctuations with a help of a phase detector. In the scheme, the phase detector is calibrated by a photonic-assisted MPS. In conventional methods, the phase shift was achieved by an electrical phase shifter, which generally has narrow bandwidth and heavy weight. Therefore, we make use of a photonic-assisted MPS to achieve a larger working bandwidth. We firstly demonstrate the wideband property of the photonic-assisted MPS with an assist of an electrical vector network analyzer (EVNA) to measure its phase and magnitude responses. Meanwhile, we measure the NPD of the proposed phase noise analysis method induced by higher-order sidebands.

## III. EXPERIMENT AND RESULT

We carried out an experiment to verify the proposed phase noise analysis method based on the setup shown in Fig. 1. An optical carrier emitted at 1550.118 nm from a LD was fiber-coupled into a DPMZM. The output power of the LD was fixed at 173.4 mW. The DPMZM has a bandwidth of 40 GHz and a half-wave voltage of 3.5 V for its sub-MZMs and 16 V for its parent MZM. A DC extinction ratio for each sub-MZM was more than 20 dB. One of RF ports of the DPMZM was driven by a microwave signal generated from an OUT at the fixed output
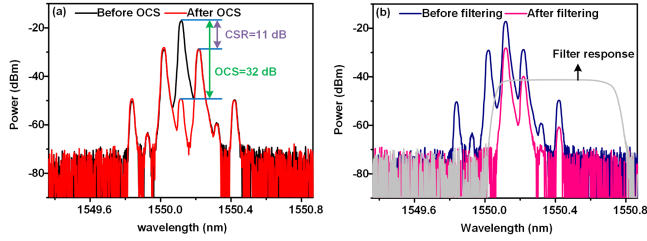
Fig. 3. Measured optical spectra (a) at the output of the DPMZM, (b) before and after the OBPF and the transmission response of the OBPF.
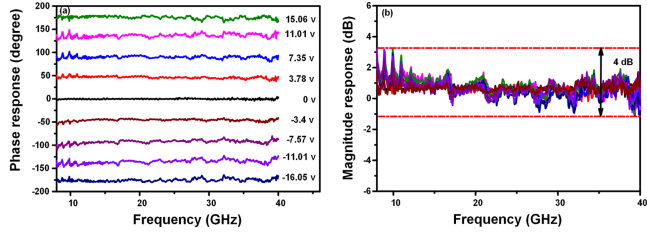


Fig. 4. (a) Measured phase response and (b) and power variation of the phase noise analysis system when the bias voltage $V_3$ is tuning from $-16.05$ V to $15.06$ V, respectively.
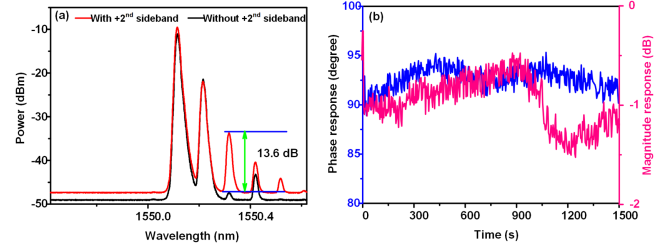


Fig. 5. (a) Optical spectra with and without second order sidebands, (b) magnitude and phase long-term stability measurement.



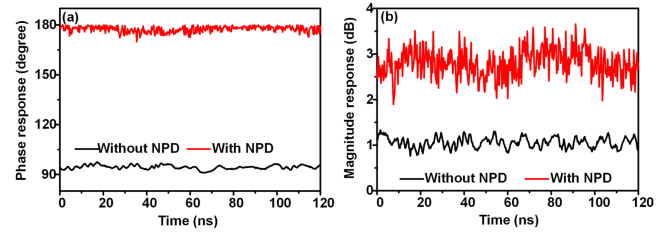Fig. 6. Comparison of output (a) phase and (b) intensity responses with and without NPD.

power of 0 dBm. An EA with a 3-dB bandwidth from 40 kHz to 38 GHz, and a gain of 23 dB were inserted between the LD and the DPMZM to boost the microwave signal power up to 23 dBm. In order to verify the performance of the photonic-assisted MPS, an EVNA with a working bandwidth from 50 MHz to 40 GHz was used to measure its phase and magnitude responses. An OBPF attached after the DPMZM was used to remove either sideband of the optical carrier and its bandwidth was set at 650 pm. The modulated optical signal was then sent into a PD with a bandwidth of 40 GHz. The electrical mixer acting as a phase detector has a LO and an RF bandwidth from DC to 14 GHz and an IF bandwidth from DC to 8 GHz. LNA1 and LNA1 were used to amplify the electrical signal power to ensure the mixer working at a saturated condition. First, we set the bias voltages of the two sub-MZMs at $V_1=V_2=V_\pi=3.5$ V to make them working at the MITP to suppress optical carrier as shown in the red line in Fig. 3(a), which is recorded by an optical spectrum analyzer (OSA) with a resolution of 0.01 nm. As can be seen from Fig. 3(a), the optical carrier suppression ratio could reach more than 32 dB. Then, we tuned the bias voltage of MZM2 $V_2=0$ V to pass through a pure optical carrier as shown in a black line in Fig. 3(a). The OCSR is 11 dB. Fig. 3(b) shows optical spectra before and after the OBPF and the transmission response of the OBPF when the frequency of the driven signal was 12 GHz.

In order to demonstrate the wideband property of the proposed phase noise analysis system, we measured phase and magnitude response of the system with a help of an EVNA. Fig. 4(a) shows the measured phase response by adjusting the bias voltage $V_3$ after a calibration process at $V_3=0$ V, and it was done in advance to remove an inherent system response. It is obviously that the phase of the microwave signal under test could be continuously tuned over a full $360°$. Fig. 4(b) shows the corresponding

magnitude response. As can be seen from Fig. 4(b), the magnitude of the microwave signal under test could be retained a constant over a wide bandwidth.

Meanwhile, we investigated the NPD induced by the photonic-assisted MPS. As mentioned in principle, the undesirable higher order modulated sidebands will induce the NPD. In this case, the bias voltage $V_1$ was tuned to be 1.71 V to make MZM1 work at linear modulation condition and the bias voltage $V_2$ was then adjusted to be 2.7 V to control the optical carrier power constant. Fig. 5(a) shows the optical spectra with and without second order sidebands. It is clearly that the second order sideband was increased by 13 dB after adjusting bias voltages $V_1$ and $V_2$, and other sidebands keep almost constant.

As depicted in Fig. 6, a comparison was made between the phase and magnitude responses of the output with and without NPD at a fixed $90°$ phase shift. The results indicated that the phase and intensity responses of the MPS output were greatly optimized in the absence of NPD. For phase responses, the relatively phase difference is meaningful which implies that undesirable higher order sidebands generate some extra fundamental frequency microwave signals to overlap with the wanted microwave signal. The additionally generated signals will have a vector resultant to distort the phase and magnitude of the microwave signals. It is worth noting, for the conditions, the bias voltage $V_3$ kept unvaried at the value of 7.59 V and the microwave power kept constant.

System stability broken into long-term stability and short-term stability is a pretty important issue for the whole system [27]. In the proposed system, the photonic-assisted microwave processor is much more sensitive than other parts. Therefore, we measured a phase and magnitude stability of the generated microwave signal at the PD output as shown in Fig. 5(b). It can be seen that the phase deviation over time duration of more than 1500 s is less than $5°$ and amplitude
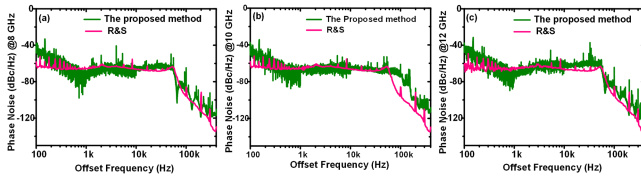
Fig. 7.   Measured phase noise of microwave signals at the frequency of (a) 8 GHz; (b) 10 GHz, and (c) 12 GHz.

variation is less than 1 dB. The experimental results indicate that the microwave signal after processing by the photonic techniques has a good long term stability performance. To verify the feasibility of the proposed method, phase noise of microwave signals at 8-, 10-, 12-GHz carrier was measured. During the measurements, only $V_3$ was adjusted when frequency of the microwave signals under test was changed. The dispersion of the SMF and the DCF are 17 and $-169$ ps/(nm.km), respectively. In total, the splice loss of the DCSMF is about 3.05 dB. The length of the DCSMF is about 3 km and the corresponding delay time is about 15 $\mu$s. The nonlinear threshold power for the DCSMF is about 12 dBm. In the experiment, the power of the optical signals put into the DCSMF was strictly limited to avoid some nonlinear effects such as stimulated Brillouin scattering (SBS) and self-phase modulation (SPM). Meanwhile, the OCSR was tuned to achieve the optimal dynamic range for the system. The experimental results are shown in Fig. 7. As a comparison, the phase noise was also measured by a commercial phase noise analyzer from Rohde&Schwarz (R&SFSWP50). At a frequency offset of 10 kHz, the phase noise with $-66.7$ dBc/Hz at 8 GHz carrier, $-65.5$ dBc/Hz at 10 GHz carrier, and $-62.1$ dBc/Hz at 12 GHz carrier was measured with the proposed method, respectively. At a frequency offset of 1 kHz, the phase noise levels for the 8 GHz, 10 GHz, and 12 GHz carriers were $-70.8$ dBc/Hz, $-66.3$ dBc/Hz, and $-64.1$ dBc/Hz, respectively. It is clearly shown that two curves in Fig. 7 approximately agree with each other. The phase noise differences between two curves at offset frequencies lower than 250 Hz is relatively obvious, and the measured phase noise curve using the proposed method almost linearly increases below the 1 kHz offset frequency. We analyzed the phase noise property based on power-law relationship of phase noise in a function of Fourier frequency in the log-log scale. The observed disparities in the measurements can be attributed to the presence of flicker noise stemming from the LNAs and the PD during the phase noise measurement process [28]. It's worth noting that the measured phase noise curve exhibits a dip at around 66 kHz, followed by regular dips, which is attributed to the transmission response of the DCSMF. The location of the first dip in the phase noise curve determines the upper frequency limit of our proposed phase noise analysis method, following the relation $f = 1/\tau$. According to prior research [9], measurement results within a frequency offset range of approximately $f < 0.95/\tau$ are considered reliable.

## IV. CONCLUSION

We have proposed and experimentally demonstrated a high precision phase noise analysis method based on a photonic-assisted MPS without NPD using a DPMZM. The key photonic units of the proposed method are the photonic-assisted MPS and a DCSMF acting as the photonic delay line. The phase tuning property over a wide bandwidth of the proposed method is firstly experimentally demonstrated. Moreover, we experimentally measured the NPD and the long-term stability of the proposed system. Microwave signals at the frequency of 8-, 10-, and 12- GHz with phase noise of $-66.7$, $-65.5$, and $-62.1$ dBc/Hz at 10 kHz offset frequency were experimentally measured, respectively.

## REFERENCES

[1] D. B. Leeson, "Oscillator phase noise: A 50-year review," *IEEE Trans. Ultrason., Ferroelectr., Freq. Control*, vol. 63, no. 8, pp. 1208–1225, Aug. 2016.

[2] A. K. Poddar, U. L. Rohde, and A. M. Apte, "How low can they go?: Oscillator phase noise model, theoretical, experimental validation, and phase noise measurements," *IEEE Microw. Mag.*, vol. 14, no. 6, pp. 50–72, Sep./Oct. 2013.

[3] T. Hao et al., "Optoelectronic parametric oscillator," *Light: Sci. Appl.*, vol. 9, no. 1, 2020, Art. no. 102.

[4] K. Siddiq, R. J. Watson, S. R. Pennock, P. Avery, R. Poulton, and B. Dakin-Norris, "Phase noise analysis in FMCW radar systems," in *Proc. Eur. Microw. Conf.*, 2015, pp. 1523–1526.

[5] M. Nebel and B. Lankl, "Oscillator phase noise as a limiting factor in stand-alone GPS-indoor navigation," in *Proc. 5th ESA Workshop Satell. Navigation Technol. Eur. Workshop GNSS Signals Signal Process.*, 2010, pp. 1–8.

[6] A. G. Armada and M. Calvo, "Phase noise and sub-carrier spacing effects on the performance of an OFDM communication system," *IEEE Commun. Lett.*, vol. 2, no. 1, pp. 11–13, Jan. 1998.

[7] U. L. Rohde, A. K. Poddar, and A. M. Apte, "Getting its measure: Oscillator phase noise measurement techniques and limitations," *IEEE Microw. Mag.*, vol. 14, no. 6, pp. 73–86, Sep./Oct. 2013.

[8] R. Jauregui and J. Portilla, "Optimum-setting and calibration procedures for heterodyne measurements of amplitude and phase noise in high-frequency amplifiers," *IEEE Trans. Microw. Theory Techn.*, vol. 62, no. 5, pp. 1239–1248, May 2014.

[9] E. Rubiola, E. Salik, S. Huang, N. Yu, and L. Maleki, "Photonic-delay technique for phase-noise measurement of microwave oscillators," *J. Opt. Soc. Amer. B*, vol. 22, no. 5, pp. 987–997, 2005.

[10] K. Jung and J. Kim, "All-fibre photonic signal generator for attosecond timing and ultralow-noise microwave," *Sci. Rep.*, vol. 5, no. 1, 2015, Art. no. 16250.

[11] Y. Xie, P. Zhou, Z. Jiang, Z. Zhou, Z. Song, and N. Li, "A compact photonic-delay line phase noise measurement system based on an electro-absorption modulated laser," in *Proc. Photon. Electromagn. Res. Symp.*, 2021, pp. 801–804.

[12] N. Kuse and M. Fermann, "Electro-optic comb based real time ultra-high sensitivity phase noise measurement system for high frequency microwaves," *Sci. Rep.*, vol. 7, no. 1, 2017, Art. no. 2847.

[13] J. Shi, F. Zhang, D. Ben, and S. Pan, "Wideband microwave phase noise analyzer based on an all-optical microwave I/Q mixer," *J. Lightw. Technol.*, vol. 36, no. 19, pp. 4319–4325, Oct. 2018.

[14] F. Zhang, J. Shi, and S. Pan, "Wideband microwave phase noise measurement based on photonic-assisted I/Q mixing and digital phase demodulation," *Opt. Exp.*, vol. 25, no. 19, pp. 22760–22768, 2017.

[15] J. Shi, F. Zhang, and S. Pan, "Phase noise measurement of RF signals by photonic time delay and digital phase demodulation," *IEEE Trans. Microw. Theory Techn.*, vol. 66, no. 9, pp. 4306–4315, Sep. 2018.

[16] D. Zhu, F. Zhang, P. Zhou, D. Zhu, and S. Pan, "Wideband phase noise measurement using a multifunctional microwave photonic processor," *IEEE Photon. Technol. Lett.*, vol. 26, no. 24, pp. 2434–2437, Dec. 2014.

[17] D. Zhu, F. Zhang, P. Zhou, and S. Pan, "Phase noise measurement of wideband microwave sources based on a microwave photonic frequency down-converter," *Opt. Lett.*, vol. 40, no. 7, pp. 1326–1329, 2015.

[18] W. Wang, J. G. Liu, H. Mei, W. Sun, and N. Zhu, "Photonic-assisted wideband phase noise analyzer based on optoelectronic hybrid units," *J. Lightw. Technol.*, vol. 34, no. 14, pp. 3425–3431, Jul. 2016.

[19] Y. Xie, P. Zhou, Z. Jiang, and N. Li, "Wideband phase noise measurement of microwave signals based on all-optical microwave signal processing," in *Proc. IEEE 20th Int. Conf. Opt. Commun. Netw.*, 2022, pp. 1–3.

[20] Z. Jiang, P. Zhou, R. Zhang, K. Li, and N. Li, "Photonics-based dual-functional system for microwave signal generation and phase noise measurement," in *Proc. Asia Commun. Photon. Conf.*, 2021, Paper T3E–4.

[21] F. Zhang, D. Zhu, and S. Pan, "Photonic-assisted wideband phase noise measurement of microwave signal sources," *Electron. Lett.*, vol. 51, no. 16, pp. 1272–1274, 2015.

[22] Y. Xie, P. Zhou, Z. Jiang, Z. Zhou, and N. Li, "Wideband microwave phase noise analyzer based on all-optical microwave signal processing," *IEEE Photon. J.*, vol. 14, no. 4, Aug. 2022, Art. no. 5538706.

[23] W. Wang et al., "A wideband photonic microwave phase shifter using polarization-dependent intensity modulation," *Opt. Commun.*, vol. 356, pp. 522–525, 2015.

[24] J. Capmany and D. Novak, "Microwave photonics combines two worlds," *Nature Photon.*, vol. 1, no. 6, pp. 319–330, 2007.

[25] W. Li, W. H. Sun, W. T. Wang, L. X. Wang, J. G. Liu, and N. H. Zhu, "Photonic-assisted microwave phase shifter using a DMZM and an optical bandpass filter," *Opt. Exp.*, vol. 22, no. 5, pp. 5522–5527, 2014.

[26] J. Yao, "Microwave photonics," *J. Lightw. Technol.*, vol. 27, no. 3, pp. 314–335, Feb. 2009.

[27] J. Yang, E. H. Chan, X. Wang, X. Feng, and B. Guan, "Broadband photonic microwave phase shifter based on controlling two RF modulation sidebands via a Fourier-domain optical processor," *Opt. Exp.*, vol. 23, no. 9, pp. 12100–12110, 2015.

[28] O. Okusaga, W. Zhou, E. Levy, M. Horowitz, G. Carter, and C. Menyuk, "Non-ideal loop-length-dependence of phase noise in OEOs," in *Proc. Conf. Lasers Electro- Opt.*, 2009, Paper CFB3.